

# Detecting regular dynamics from time series using permutations slopes

J. S. Armand Eyebe Fouda<sup>a</sup>, Wolfram Koepf<sup>b</sup>

<sup>a</sup>*Department of Physics, Faculty of Science, University of Yaoundé I, P.O. Box 812, Yaoundé, Cameroon*

<sup>b</sup>*Institute of Mathematics, University of Kassel, Heinrich-Plett Str. 40, 34132 Kassel, Germany*

---

## Abstract

In this paper we present the entropy related to the largest slope of the permutation as an efficient approach for distinguishing between regular and non-regular dynamics, as well as the similarities between this method and the three-state test (3ST) algorithm. We theoretically establish that for suitably chosen delay times, permutations generated in the case of regular dynamics present the same largest slope if their order is greater than the period of the underlying orbit. This investigation helps making a clear decision (even in a noisy environment) in the detection of regular dynamics with large periods for which PE gives an arbitrary nonzero complexity measure.

*Keywords:* time series analysis, ordinal patterns, chaos detection, entropy

---

## 1. Introduction

Complexity measure is important as it allows comparing time series and distinguishing between regular (e.g. periodic) and non-regular behaviors. A deterministic dynamical system generating non-regular dynamics is said to be chaotic. Detecting chaos from an arbitrary series of observations remains a challenging task [1–6], as it is difficult to make a clear difference between the deterministic chaotic and stochastic dynamics. Some investigations have been carried out in this area and are still giving promising results [7–9]. If the system is assumed to be deterministic, measuring its complexity is useful for determining whether its behavior is predictable or not. Entropies, fractal dimension and Lyapunov exponent (LE) are some examples of complexity parameters.

Particular interest has been reserved to entropies as some of them can be directly applied to the series of observations [1, 10–14]. In this perspective, Bandt and Pompe have proposed the permutation entropy (PE) [1], which is actually widely used in many fields due to its conceptual and computational simplicity. The PE is based on the ordinal pattern analysis and is easily calculated for any type of time series, be it regular, chaotic, noisy, or reality based. It has been

---

*Email addresses:* [efoudajsa@yahoo.fr](mailto:efoudajsa@yahoo.fr), Tel: +23770836099 (J. S. Armand Eyebe Fouda), [koepf@mathematik.uni-kassel.de](mailto:koepf@mathematik.uni-kassel.de) (Wolfram Koepf)  
*URL:* <http://www.mathematik.uni-kassel.de/~koepf/> (Wolfram Koepf)

successfully applied to the study of structural changes in time series and the underlying system dynamics [15–19]. In addition to its robustness against noise, it has been verified that the PE behaves similar to the largest Lyapunov exponent and can therefore be used for the detection of chaos in dynamical systems [20].

However, although regular dynamics present vanishing or negligible complexities, there is no particular value or property of the PE for the characterization of regular dynamics as it is the case for the largest LE, which makes it less suitable for chaos detection. Indeed, in some examples given on chaos detection, PE tracks the largest LE with a uniform bias that depends on the underlying system and the parameter setting of the PE algorithm: even perfectly predictable dynamics are characterized by a nonzero entropy. The dependence on the uniform bias can be sometimes difficult to determine when dealing with an unknown single time series. Despite the modification proposed by the weighted PE [21] and the modified PE [22] algorithms to overcome some shortcomings of the PE, no solution has been proposed to address this concern. For the PE algorithm to be efficiently implemented, a principle based on the use of lookup tables was presented in [23]. Defining lookup tables for large permutation order  $n$  is difficult as the number of permutations is equal to  $n!$ . In the case of the modified PE, the number of permutations is given by the *ordered Bell numbers*, which is greater than  $n!$  [23]. Thus approximating the Kolmogorov-Sinai (KS) entropy from the PE is quite difficult as it requires large  $n$ . Moreover, defining a lookup table may not be useful if the algorithm is implemented for embedding systems. Recently the conditional entropy of ordinal patterns was proposed that provides more reliable estimation of the KS entropy [24] than the PE.

In 2004, Gottwald and Melbourne proposed the 0-1 test for chaos detection from time series. The test presents the advantage to be binary as it outputs 0 for regular dynamics and 1 for non-regular dynamics. The 0-1 test has shown competitive results and has been successfully applied to many types of dynamical systems and experimental data [25–27]. The test is still in improvement and has been recently slightly modified for an efficient application to strange non-chaotic attractors (SNA) [28]. The 0-1 test is sensitive to the sampling frequency. Gottwald and Melbourne showed that in the case of continuous time systems, it fails to detect chaos in oversampled time series, hence it is necessary to reduce the sampling frequency to the Nyquist frequency. However, such a condition is not consistent with the digital signal processing requirement for which the sampling frequency needs to be greater than the Shannon limit. In order to overcome such a limiting property, we proposed the modified 0-1 test in which the 0-1 test is applied to the local maxima and minima of the observations, instead of directly applying to the entire observation [29]. The modified 0-1 test thus allows to easily detect chaos from oversampled time series. However, despite this improvement, the 0-1 test remains computationally costly and cannot be used for real-time analysis of time series as it is the case for the PE. Moreover, the calibration of the test sometimes depends on the system under study.

Without prior knowledge on the PE, we proposed another approach for time series analysis, namely the three-state test (3ST) for chaos detection in discrete maps, which also belongs to the group of ordinal pattern analysis methods [30]. The 3ST presents the advantage to perform both the detection of the regularity or non-regularity and the period estimation in time series. The difference between the PE and the 3ST comes from the statistical exploitation of the

permutations. Indeed, instead of constructing ordinal patterns (permutations) of fixed order  $n$  like in the PE, in the 3ST, data sequences are ordered using different values of  $n$  and the corresponding permutations are studied. By this approach, no probability is computed as the permutations do not have the same length. Moreover, the permutation list may be very large, depending on the length of the time series, hence it has memory and computationally expensive. For this purpose, each permutation is replaced by its largest slope  $S$ . The 3ST can easily detect the period-doubling route and output the corresponding periods as discrete numbers (periods of stable limit-cycles) [30]. In addition, as an ordinal method for time series analysis, the 3ST is also computationally low cost and was designed for possible real-time applications. Recently, we proposed an improvement of the 3ST for clear discrimination between periodic, quasi-periodic and chaotic dynamics [31]. We thus defined  $\lambda_P$  as the sensitivity of the 3ST chaos indicator, namely  $\lambda$ , to the initial phase. We also showed that  $\lambda_P$  is equivalent to computing  $\lambda$  using permutations with fixed order [31]. By this definition, the 3ST and the PE appear closer, even if only the largest slopes of permutations and no probabilistic approach are used in the 3ST algorithm. However, the fundamental question is to know whether the use of the largest slopes is reliable for chaos detection.

In this paper, we theoretically prove the usefulness of the permutation slopes for the discrimination between regular and non-regular dynamics. We further establish the relationship between the 3ST and the PE by computing the entropy related to the permutations largest slopes, and show that it can be efficiently applied to the detection of chaos in dynamical systems.

## 2. Mathematical fundamentals

### 2.1. Usefulness of the permutations slopes

Let  $\{x_t\}_{t=1,\dots,T}$  be a time series of length  $T$  where  $t$  is the time index. The PE of order  $n$  is defined as a measure of the probabilities of permutations of order  $n$  [1]. Permutations of order  $n$  are obtained from the comparison of neighboring values (increasing order) in embedding vectors  $\mathbf{x}_t = (x_{t+1}, x_{t+1+\tau}, \dots, x_{t+1+m\tau}, \dots, x_{t+1+(n-1)\tau})$ , where  $n$  is the embedding dimension (number of values in  $\mathbf{x}_t$ ),  $\tau$  the distance between two values in  $\{x_t\}$  or delay time of samples and  $m+1$  the index of  $x_{t+1+m\tau}$  in  $\mathbf{x}_t$ ,  $m \in \mathbb{N}$ . Let  $P_t$  be the permutation derived from  $\mathbf{x}_t$ .  $P_t = \left(\frac{1,2,3,\dots,n}{5,n,1,\dots,3}\right)$ , for example is obtained by sorting the values of  $\mathbf{x}_t$  in ascending order, with  $x_{t+5} < x_{t+n} < x_{t+1} < \dots < x_{t+3}$ . Identical values are sorted by the ascending order of their time index. The permutation entropy of order  $n$  is thus given by

$$H(n) = - \sum p(\theta) \cdot \ln(p(\theta)) \quad (1)$$

where

$$p(\theta) = \frac{\#\{t \mid t \leq T - n, P_t = \theta\}}{T - n + 1} \quad (2)$$

is the probability of the permutation  $\theta$  and  $\#$  denotes number [1].

#### Definition 1:

A time series  $\{x_t\}$  is called period- $L$  cycle or simply  $L$ -periodic, if there exists a basic pattern of length  $q$  samples containing  $L$  distinct values ( $L \leq q$ )

periodically repeated, independently of the time origin.  $q$  is known as the time space period and  $L$  as the phase space period.

Despite the efficiency of the PE as complexity measure, it remains unsuited for distinguishing between regular and non-regular dynamics. Indeed, obtaining  $H(n) = 0$  for regular dynamics requires large embedding dimensions  $n$  and an observation time  $T \gg n!$ . Such a requirement is difficult to achieve as the memory space cannot be infinitely large. Therefore  $n$  is reduced to small values ( $2 \leq n \leq 15$ ) [1]. As a consequence,  $H(n) \neq 0$  even for perfectly predictable dynamics. It is evident that a regular dynamics cannot be detected as periodic unless the observation time is greater than its period [24, 29]. Let  $q$  be the period of the underlying dynamics, if  $n < q$ , then the corresponding PE is greater than zero. It then appears from the above restriction that only dynamics with periods less than 15 samples may be detected with zero entropy. Moreover, for a regular dynamics to be detected with zero entropy, all the embedding vectors  $\mathbf{x}_t$  should output the same permutation, which is possible only if the dynamics is a period-1 cycle, otherwise the embedding vectors will output different permutations so that the entropy of the whole dynamics is different from zero. For example, let us consider a period-5 cycle orbit obtained by generating 5 distinct random numbers (0.8147, 0.9058, 0.1270, 0.9134, 0.6324) and repeating this basic sequence  $M$ -times ( $M > 2$ ). The first four 6-order permutations obtained by sorting values of vectors  $\mathbf{x}_t$ ,  $t=0$  to 3, are the following:  $P_0 = \left(\frac{1,2,3,4,5,6}{3,5,1,6,2,4}\right)$ ;  $P_1 = \left(\frac{1,2,3,4,5,6}{2,4,5,1,6,3}\right)$ ;  $P_2 = \left(\frac{1,2,3,4,5,6}{1,6,3,4,5,2}\right)$  and  $P_3 = \left(\frac{1,2,3,4,5,6}{5,2,3,4,1,6}\right)$ . This example shows that the entropy related to the permutation (PE) is different from zero as there are at least four different permutations, although the dynamics is regular. It appears that the permutations are sensitive to the initial phase/condition, and therefore cannot efficiently help for detecting periodic dynamics as regular.

**Definition 2:**

Assuming the permutation  $P_t$  is a piece-wise linear function, we simply consider as slope of each linear function the difference  $s_i = P_t(i+1) - P_t(i)$ ,  $1 \leq i \leq n-1$ , between pairs of neighboring values in  $P_t$ . For a permutation  $P_t$  of order  $n$ , the maximum number of distinct slopes is  $n-1$ . We define as largest slope of  $P_t$ ,  $S_t = \max(\{s_i\})$  the maximum value of  $\{s_i\}$ . We showed that  $L = \lim_{n \rightarrow \infty} |S_t|$  for regular dynamics [30, 31].

**Theorem 1:**

*$n$ -order permutations generated using ascending order of the values of  $n$ -length embedding vectors  $\mathbf{x}_t$  derived from a period- $L$  cycle time series  $\{x_t\}$ ,  $L = q$ ,  $n > \frac{L}{\gcd(L,\tau)}$ , all present the same largest slope  $S = \frac{L}{\gcd(L,\tau)}$ .*

**Proof:**

$\mathbf{x}_t = (x_{t+1}, x_{t+1+\tau}, \dots, x_{t+1+m\tau}, \dots, x_{t+1+(n-1)\tau})$  outputs permutations  $P_t$  of order  $n$  after sorting in ascending order. Extracting samples from a periodic time series with a fixed step leads to another periodic sequence.

If  $\gcd(L, \tau) = 1$  and  $n \leq L$ , all the differences  $P_t(i+1) - P_t(i)$ ,  $i = 1$  to  $n-1$  can take any value between 1 and  $n-1$ , depending on the ordering of samples in  $\mathbf{x}_t$  and  $S < L$

If  $\gcd(L, \tau) \neq 1$ , then  $x_{t+t'} = x_{t+t'+L}$  where  $t' = m\tau + 1$ ,  $m \in \mathbb{N}$ . The corresponding indices in  $\mathbf{x}_t$  are respectively  $m+1$  and  $m+1+\delta$  with  $\delta = \frac{L}{\gcd(L,\tau)}$ . The possible number of distinct samples in  $\mathbf{x}_t$  is equal to  $\delta$ :  $\mathbf{x}_t$  is  $\delta$ -periodic. In the case  $n \leq \delta$ , none of the  $L$  distinct values of  $\{x_t\}$  is repeated in  $\mathbf{x}_t$  and

the largest slope takes any value  $S < \delta$  between 1 and  $n - 1$ , depending on the ordering of samples in  $\mathbf{x}_t$ .

If  $n > \delta$ , at least one of the possible  $\delta$  distinct samples in  $\mathbf{x}_t$  is repeated at least once. In that case,  $x_{t+1}$  is always repeated and each of its occurrence indicates the end of the previous period or the beginning of the next one. The time index of such occurrences is  $t + t'$ , where  $t' = m\tau + 1$ ,  $m$  being an integer such that  $m+1 > \delta$ . As  $\mathbf{x}_t$  is  $\delta$ -periodic, the index  $m+1$  indicating the repetition of  $x_{t+1+\alpha}$ ,  $0 \leq \alpha < \delta$ , is such that:

$$\text{mod}(m+1, \delta) = \alpha + 1 \quad (3)$$

The general solution of Eq.(3) is  $m(k) = k \cdot \delta + \alpha$ ,  $k \geq 0$  is the number of repetitions. According to the definition of  $\mathbf{x}_t$ , the largest slope  $S$  is equal to the distance between indices of successive occurrences of the same value, so  $S = m(k+1) - m(k) = \delta$ . Thus, considering the definition of  $\delta$ , the largest slope is:

$$S = \frac{L}{\text{gcd}(L, \tau)}, \quad (4)$$

hence the result.

For example the largest slopes of the above 6-order permutations  $P_0, P_1, P_2$  and  $P_3$  are  $S_0 = S_1 = S_2 = S_3 = 5$ . Each of the corresponding four vectors  $\mathbf{x}_t$ ,  $t = 0$  to 3, has the same values and differ only by the initial value. All the four different  $\mathbf{x}_t$  are period-5 sequences.

**Consequence:**

Theorem 1 shows that the estimate of the phase space period of the time series  $\{x_t\}$  by the largest slope  $S$  depends on the delay time  $\tau$ . For this estimate to be equal to  $L$ , it is necessary that  $\text{gcd}(L, \tau) = 1$ . As it is difficult to meet such a condition for arbitrary time series, choosing  $\tau = 1$  is sufficient.

In the case of the PE for example, choosing  $\tau > 1$  can lead to some misinterpretations in complexity values in the case of regular dynamics. Indeed, let us consider a 3-periodic and a 10-periodic time series. Normally, the first dynamics is less complex than the second one, but choosing  $\tau = 5$  will reduce the second dynamics into a 2-periodic one, thus leading to a smaller complexity. For  $n = 7$ , the corresponding PE are respectively  $H_1(7) = \ln(3) = 1.0986$  and  $H_2(7) = \ln(10) = 2.3026$  for  $\tau = 1$ ; and  $H_1(7) = \ln(3) = 1.0986$  and  $H_2(7) = \ln(2) = 0.6931$  for  $\tau = 5$ . This observation also proves that the bias between the PE and the largest Lyapunov exponent cannot be determined rigorously.

However, although choosing  $\tau > 1$  can lead to false results for the detection of regular dynamics periods, it can be useful for detecting regular dynamics of large period from small embedding dimensions ( $n < L$ ). Indeed, if  $\tau$  is such that  $\text{gcd}(L, \tau) > 1$ , then the period of the time series is reduced to  $\delta < L$  and choosing  $\delta < n < L$  even allows to detect the dynamics as periodic.

**Theorem 2 (Periodicity of permutations):**

*Given a period- $L$  cycle series  $\{x_t\}$  and  $\tau$  such that  $\text{gcd}(L, \tau) = 1$ , the number of distinct  $n$ -order permutations,  $n > L$ , generated from the ascending sorting of the values of  $n$ -length embedding vectors  $\mathbf{x}_t, \mathbf{x}_{t+t_0}, \dots, \mathbf{x}_{t+lt_0}$ ,  $t_0 < n$ , is equal to  $\frac{L}{\text{gcd}(L, t_0)}$ ,  $t_0$  being the delay time of the embedding vectors.*

**Proof:**

If  $t_0 = 1$ ,  $\mathbf{x}_t$  and  $\mathbf{x}_{t+L}$  according to Theorem 1 are redundant:  $\{\mathbf{x}_t\}$  is  $L$ -periodic. It then results that  $P_t$  and  $P_{t+L}$  are the same, and only  $P_t$  to  $P_{t+L-1}$  are distinct permutations. So, the set of permutations in that case is  $L$ -periodic as the time series  $\{x_t\}$ .

If  $t_0 > 1$  and  $\frac{L}{\gcd(L,t_0)} = \gamma$ , according to Theorem 1, it is easily verified that  $\mathbf{x}_t$  and  $\mathbf{x}_{t+\gamma}$  are redundant as  $\{x_t\}$  is  $L$ -periodic. So, the number of distinct permutations obtained from  $\{\mathbf{x}_{t+lt_0}\}$ ,  $l \in \mathbb{N}$ , is equal to  $\gamma$ :  $\{P_t\}$  is  $\gamma$ -periodic, hence the result.

For  $\gcd(L, \tau) > 1$ , the number of distinct permutations can be smaller than  $\gamma$ , depending on the ordering of the values in  $\{x_t\}$ : the choice of  $\tau$  can reduce the number of distinct permutations. Thus,  $\gamma$  is the maximum number of distinct permutations which can be obtained, given the couple  $(\tau, t_0)$ .

Let us consider for example a 4-periodic ( $L = 4$ ) time series such that  $\{x_t\} = \{a_0, a_1, a_2, a_3, a_0, a_1, a_2, a_3, a_0, \dots\}$ , where  $a_0 \neq a_1 \neq a_2 \neq a_3$  are real numbers; and an embedding dimension  $n = 5$ . For  $\tau = 1$  and  $t_0 = 1$ , the corresponding embedding vectors are the following:  $\mathbf{x}_0 = (a_0, a_1, a_2, a_3, a_0)$ ,  $\mathbf{x}_1 = (a_1, a_2, a_3, a_0, a_1)$ ,  $\mathbf{x}_2 = (a_2, a_3, a_0, a_1, a_2)$ ,  $\mathbf{x}_3 = (a_3, a_0, a_1, a_2, a_3)$ ,  $\mathbf{x}_4 = \mathbf{x}_0$ ,  $\mathbf{x}_5 = \mathbf{x}_1, \dots, \mathbf{x}_t = \mathbf{x}_{t-4}$ ,  $t \geq 4$ . According to this example, there are only four distinct embedding vectors, so only four distinct permutations can be observed ( $\gamma = \frac{L}{\gcd(L,t_0)} = 4$ ) and all of them have the same largest slope equal to the period of the time series,  $S = L = \frac{L}{\gcd(L,\tau)} = 4$ .

Now let us consider  $\tau = 2$  and  $t_0 = 1$ , the embedding vectors become:  $\mathbf{x}_0 = (a_0, a_2, a_0, a_2, a_0)$ ,  $\mathbf{x}_1 = (a_1, a_3, a_1, a_3, a_1)$ ,  $\mathbf{x}_2 = (a_2, a_0, a_2, a_0, a_2)$ ,  $\mathbf{x}_3 = (a_3, a_1, a_3, a_1, a_3)$ ,  $\mathbf{x}_4 = \mathbf{x}_0$ ,  $\mathbf{x}_5 = \mathbf{x}_1, \dots, \mathbf{x}_t = \mathbf{x}_{t-4}$ ,  $t \geq 4$ . Once more, the number of distinct embedding vectors is equal to 4; but the number of distinct permutations depends on the ordering of the samples in the time series. For the case  $a_0 < a_2 < a_3 < a_1$ , there are only two distinct permutations:  $P_0 = P_3 = \begin{pmatrix} 1,2,3,4,5 \\ 1,3,5,2,4 \end{pmatrix}$  and  $P_1 = P_2 = \begin{pmatrix} 1,2,3,4,5 \\ 2,4,1,3,5 \end{pmatrix}$ , which is less than  $\gamma = \frac{L}{\gcd(L,t_0)} = 4$  permutations. However, the largest slope of the permutations now is half the period of the time series,  $S = \frac{L}{\gcd(L,\tau)} = 2$ .

By setting  $\tau = 1$  and  $t_0 = 2$ , the embedding vectors are the following:  $\mathbf{x}_0 = (a_0, a_1, a_2, a_3, a_0)$ ,  $\mathbf{x}_2 = (a_2, a_3, a_0, a_1, a_2)$ ,  $\mathbf{x}_4 = \mathbf{x}_0$ ,  $\mathbf{x}_6 = \mathbf{x}_2, \dots, \mathbf{x}_{2t} = \mathbf{x}_{2t-4}$ ,  $t \geq 2$ . It then comes that the maximum number of distinct permutations is now half the period of the time series:  $\gamma = \frac{L}{\gcd(L,t_0)} = 2$ ; while the largest slope of these permutations remains  $S = L = 4$ .

Finally, if  $\tau = 2$  and  $t_0 = 2$ , the embedding vectors are:  $\mathbf{x}_0 = (a_0, a_2, a_0, a_2, a_0)$ ,  $\mathbf{x}_2 = (a_2, a_0, a_2, a_0, a_2)$ ,  $\mathbf{x}_4 = \mathbf{x}_0$ ,  $\mathbf{x}_6 = \mathbf{x}_2, \dots, \mathbf{x}_{2t} = \mathbf{x}_{2t-4}$ ,  $t \geq 2$ . It now clearly appears that both the number of permutations and the largest slopes are reduced to half the period of the time series.

This example can be extended to any period to see the interplay between  $\tau$  and  $t_0$

### Consequences:

**C1:** Theorem 2 shows that only  $\gamma$  ( $\gamma \leq L < n$ ) permutations are periodically repeated in the case of regular dynamics, instead of  $n!$ . This number is less than or equal to the possible number of largest slopes, so the permutations can be efficiently represented by their largest slopes with no information loss. In addition, for a given regular dynamics, all the  $\gamma$  permutations have the same largest slope.

On the contrary, for non-regular dynamics if the period  $L$  is assumed to be infinitely large, then  $n < L$  implies that the number of distinct permutations is greater than  $n$ . Therefore the permutations cannot be efficiently described by the  $n - 1$  possible values of largest slopes any more. It then results that for a given dynamics, there is more than a single value of largest slope as in the case of regular dynamics.

From the above consequences, we can conclude that regular dynamics can be characterized by a single largest slope while non-regular dynamics cannot. This difference can help to distinguish between the two types of dynamics. The largest slopes do not allow to represent all the possible permutations in the case of non-regular dynamics and therefore are not useful for estimating their complexity.

**C2:** Theorem 2 shows that the number of distinct permutations is less than or equal to  $L$  and that  $\{P_t\}$  is  $\gamma$ -periodic. This proof implies that there is no need to consider large observation durations, as the periodicity of the permutations can be detected from only three to four cycles. So, the effective observation time can be set such that  $3n \leq T \leq 4n$ , with  $n > L_m$  the largest period to be estimated without error. This observation also implies that only  $3\gamma$  to  $4\gamma$  permutations can be sufficient for the detection to be accurate. When  $t_0$  is chosen such that  $\gcd(L, t_0) > 1$ ,  $4\gamma$  can be too small and allows to save more computation time.

Indeed, considering the largest slope does not allow us to determine the complexity, but only to distinguish between regular and non-regular dynamics. So, it is not useful any more to consider  $T \gg n!$ , but only  $T > 3n$ . This observation is as important as it can help speeding up the detection of the regularity of dynamics for real-time applications, and to make a clear decision from a small amount of data. For low-dimensional systems for example, where periodic dynamics present few number of harmonics,  $T$  can be too short as  $n$  can be too small.

**Remarks:**

**R1:** In the case  $L = q$  and  $n < L$ , the set of largest slopes  $\{S_t\}$  derived from  $\{\mathbf{x}_t\}$  is  $\gamma$ -periodic. Indeed, for any embedding dimension  $n < L$ , the embedding vectors  $\mathbf{x}_t$  are periodically repeated as the time series  $\{x_t\}$  is  $L$ -periodic, even if the largest slopes of the corresponding permutations  $P_t$  take possible values between 1 and  $n - 1$ , depending on the ordering of the values in  $\{x_t\}$ . Theorem 2 shows that embedding vectors  $\mathbf{x}_t$  are periodically repeated and only a maximum of  $\gamma$  distinct permutations  $P_t$  can be derived from such embedding vectors. The number of distinct permutations for a regular dynamics does not explicitly depend on the embedding dimension, but only on  $L$ ,  $t_0$ ,  $T$  and the ordering of the values. As stated above, the time period of  $\{S_t\}$  is equal to  $\gamma$ , similar as that of  $\{\mathbf{x}_t\}$ , except when all the  $S_t$  values are the same. In such a case,  $\{S_t\}$  corresponds to a period-1 cycle time series. As only a maximum of  $\gamma$  distinct permutations can be derived from the set of embedding vectors  $\mathbf{x}_t$ , although the corresponding largest slopes may be different, it can be conjectured that the upper limit of the PE of a  $L$ -periodic dynamics is  $\ln(\gamma)$ , where  $\gamma = \frac{L}{\gcd(L, t_0)}$ . This limiting value is obtained when all the  $\gamma$  permutations are realized with the same probability. The dependence of the number of distinct permutations on the ordering of values in  $\{x_t\}$  and  $\tau$  can lead to arbitrary nonzero values of the PE for regular dynamics: two regular dynamics with the same period can

give different permutation entropies.

**R2:** In the case  $L < q$ , redundant values occur in the basic period of  $\{x_t\}$ . For the largest slope to be unique and equal to  $q$ , at least one non-redundant value should be repeated in  $\mathbf{x}_t$ . For avoiding any detection error, it is necessary to consider the time period as it remains constant even for embedding vectors with redundant values ( $L < q$ ). This requirement can be easily justified by considering  $n \geq 2q$  as embedding dimension. For example,  $n = 200$  is enough for detecting dynamics with period  $q = 100$ . In the case there is no redundant value, even period  $q = 199$  can be efficiently detected with  $n = 200$ .

## 2.2. Permutation largest slope entropy

Theorems 1 and 2 indicate that  $L$ -periodic dynamics are characterized by a single value of largest slope if the embedding dimension is such that  $L < n$ . It then results that the entropy related to the distribution of the largest slopes may be equal to zero in the case of regular dynamics, so useful for their detection as compared to the PE which is taking arbitrary values. Thus, we define the *permutation largest slope entropy* (PLSE) of order  $n \geq 2$  as:

$$H_S(n) = - \sum p(S) \ln(p(S)) \quad (5)$$

where

$$p(S) = \frac{\#\{t \mid t \leq T - n, S_t = S\}}{T - n + 1} \quad (6)$$

is the probability/ relative frequency of  $S$  and  $\#$  denotes number.  $H_S(n) = 0$  for regular dynamics with period  $L < n$  and  $0 < H_S \leq \ln(n - 1)$  for non-regular dynamics. We can also define the normalized PLSE as:

$$h_S(n) = H_S(n) / \ln(n - 1). \quad (7)$$

$h_S(n) = 0$  for regular dynamics and  $0 < h_S(n) \leq 1$  for non-regular dynamics. Indeed, regular dynamics are characterized by a single value of largest slope  $S_t = S$ , for all  $t$  and  $H_S = 0$  as  $p(S) = 1$ ; for non-regular dynamics,  $S_t$  takes different values, thus leading to a nonzero entropy. By this approach, the PLSE can help to distinguish between regular and non-regular dynamics.

The definition of the entropy related to  $S_t$  allows to reduce redundant permutations in the case of regular dynamics: two permutations with the same largest slope are equivalent. The maximum number of permutations with different largest slopes is thus  $n - 1$  instead of  $n!$ .

## 2.3. Relationship between the 3ST and the PLSE

We defined the 3ST algorithm for distinguishing between regular and non-regular dynamics. The difference between the PLSE and 3ST resides in the statistical analysis of the largest slope. We first computed the periodicity index  $\lambda$  by considering embedding vectors of different lengths [30]. Thereafter, we studied the sensitivity of  $\lambda$  to the initial phase, namely  $\lambda_P$ , by considering embedding vectors of fixed length [31]. The interpretation of  $\lambda_P$  is similar to that of the PLSE:  $\lambda_P = 0$  for regular dynamics and  $\lambda_P > 0$  for non-regular dynamics. Computing the PLSE is similar to computing  $\lambda_P$ , except that the PLSE algorithm is easy to implement.

The number of distinct permutations in the case of regular dynamics does not explicitly depend on the embedding dimension  $n$ . However, choosing  $n < L$  may lead to permutations with different largest slopes, hence to  $h_S > 0$  for regular dynamics. In order to prevent such false detection, large embedding dimensions are required. The value of  $n$  is then chosen such that  $n > L_m$ , where  $L_m$  is the largest period to be detected with no error. Periodic dynamics whose periods are greater than  $L_m$  are considered to be chaotic and the choice of  $L_m$  depends on the complexity of the system under study.

#### 2.4. The differential dynamical quantization

The PE is robust against noise and has been successfully applied to real-world data. For the PLSE to be useful for the detection of the regularity, it should take zero values for regular dynamics even in the presence of noise. As it is not always so, we suggest to use the *differential dynamical quantization* (DDQ) for noise reduction. The DDQ is a nonlinear approach which consists in affecting a single value (quantization) to those which are approximately the same in the data series. This quantization is said dynamical as it is made for each embedding vector  $\mathbf{x}_t$ : the same value appearing in  $\mathbf{x}_t$  and  $\mathbf{x}_{t+1}$  may be replaced by two different values. The *noise threshold* (or noise tolerance)  $\eta$  is used as the quantization step.  $\eta$  is the minimum difference between  $x_t$  and  $x_{t'}$  for the two values to be considered as different. The DDQ algorithm applies as follows:  $\mathbf{x}_t$  is first sorted in ascending order to obtain  $\mathbf{u}_t$  in which all equal values are neighbors; thereafter  $u_t$  and  $u_{t+1}$  are set to  $u_{t'+1}$  if  $|u_t - u_{t+1}| < \eta$  and  $t' < t$ , with  $t'$  such that  $|u_{t'} - u_{t'+1}| \geq \eta$ ; else, these values are left unchanged; finally the quantized vector  $\mathbf{v}_t$  is obtained by relocating the values of  $\mathbf{u}_t$  as in  $\mathbf{x}_t$ . Then the PLSE is applied to  $\mathbf{v}_t$ .

If for example  $\mathbf{x}_t = (2.12, 2.61, 2.53, 2.30, 2.44, 2.28)$ , then the sorted sequence is  $\mathbf{u}_t = (2.12, 2.28, 2.30, 2.44, 2.53, 2.61)$ . Setting  $\eta = 0.04$  leads to  $\mathbf{u}_t = (2.12, 2.28, 2.28, 2.44, 2.53, 2.61)$ , and finally  $\mathbf{v}_t = (2.12, 2.61, 2.53, 2.28, 2.44, 2.28)$ . It appears that  $\mathbf{x}_t(4) = 2.30$  was noise contaminated and has been replaced by 2.28 in  $\mathbf{v}_t(4)$ . The choice of the right value of  $\eta$  depends on the noise amplitude  $\varepsilon$ .

### 3. Results and discussion

#### 3.1. Impact of $\tau$ and $t_0$ on the PE and PLSE

Readers are familiar with the rich nature of the logistic map [32]:

$$x_{t+1} = rx_t(1 - x_t). \quad (8)$$

We took 501 values of the control parameter as  $3.5 \leq r \leq 4$ , by step size  $\Delta r = 10^{-3}$ . The Feigenbaum diagram is given in Fig. 1(a) for comparison with entropies in periodic windows.

The logistic map exhibits a period doubling bifurcation for  $3.5 \leq r < 3.57$ , starting with a period-4 cycle. Fig. 1 shows that choosing  $\tau > 1$  effectively reduces the PE of regular dynamics for which  $\gcd(L, \tau) > 1$ . The PE of period-4 and period-8 cycles which are respectively  $\ln(4)$  and  $\ln(8)$  for  $\tau = 1$  are now all equal to zero for  $\tau = 8$  and less than the PE of period-3 cycle which remains equal to  $\ln(3)$  for both  $\tau = 1$  and  $\tau = 8$ . The same result is observed with the

PLSE. For example,  $r = 3.606$  corresponds to a period-20 cycle and the smallest embedding dimension for  $H_S$  to be zero is equal to 21. However, considering  $\tau = 8$  brings back this period to 5, which is less than the embedding dimension  $n = 7$ , hence  $H_S(7) = 0$  for this dynamics.

For  $t_0 = 8$ , the number of distinct permutations in the case of period-4 and 8 cycles is reduced to  $\gamma = \frac{L}{\gcd(L, t_0)} = 1$ , thus leading to  $H_S(7) = 0$ ; for all other period- $L$  cycles multiple of 8, the number of distinct permutations becomes  $\gamma = L/8$  instead of  $\gamma = L$ . This reduction of the number of permutations does not guarantee a zero value of the PLSE as  $7 < L \leq 32$  may lead to different largest slopes. For the PLSE to be zero, the embedding dimension needs to be greater than the period of the underlying dynamics:  $t_0$  does not reduce the period of the orbit, but only the number of distinct permutations. Fig. 1 also shows that complexities corresponding to  $\tau = 1, t_0 = 1$  and  $\tau = 1, t_0 = 8$  are quite the same for non-regular dynamics, while for  $t_0 = 1$  and  $\tau > 1$  an increase of the complexities is observed. This observation confirms that  $t_0 > 1$  preserves the ordering/nature of the underlying dynamics, hence its complexity, while  $\tau > 1$  does not, thus giving a more complex appearance to the dynamics than it is: we have shown in Theorem 1 that  $\tau > 1$  can lead to the reduction of the periods of regular dynamics while Theorem 2 has shown that only the number of distinct permutations can change without affecting the period of the dynamics. Considering the simulation results, we can conjecture that in the case of non-regular dynamics, choosing  $1 < t_0 < n$  does not modify the number of distinct permutations, hence the complexity measure of the dynamics. Considering  $t_0 > n$  contributes to skipping samples in  $\{x_t\}$  and may lead to false detection results. It also appears that choosing large values of  $\tau$  is a limiting factor for the chaos scaling as the PE is taking quite the same value for all the non-regular dynamics. On the other hand, choosing  $t_0 > 1$  reduces the PE of regular dynamics for which  $\gcd(L, t_0) > 1$ , while maintaining the scaling of the complexities of non-regular dynamics. Fig. 1(b) and Fig. 1(c) show that  $H_S(7) < H(7)$ , which confirms that the number of distinct permutations in the case of non-regular dynamics is effectively greater than the number of possible slopes, and therefore cannot be suitably described by the largest slopes.

The impacts of  $\tau$  and  $t_0$  to the PE and the PLSE for regular dynamics are quite antagonist. For  $t_0 = 1$ ,  $\gcd(L, \tau) > 1$  contributes to reduce the period of the underlying dynamics to  $\delta < L$ , but does not change the number of distinct permutations. It therefore results that the PLSE of regular dynamics with period  $L$  such that  $\delta < n < L$  is equal to zero, while the corresponding PE is such that  $\ln(\delta) \leq H(n) \leq \ln(L)$ . In the case  $\tau = 1$  and  $\gcd(L, t_0) > 1$ , the number of distinct permutations is reduced to  $\gamma < L$ , while the period  $L$  remains unchanged. As a consequence, the PE of  $L$ -periodic orbits is reduced to  $H(n) \leq \ln(\gamma)$  whilst their PLSE is such that  $0 \leq H_S(n) \leq \ln(n-1)$  if  $n \leq L$  and  $H_S = 0$  if  $n > L$ . We choose  $n = 7$  in Fig. 1 for comparison purposes, but this value needs to be large enough for efficient detection of regular dynamics with large periods.

### 3.2. Impact of $n$ on the detection result

Now let us consider  $n = 1024$  with  $\tau = 1, t_0 = 8$  and  $n = 32$  with  $\tau = 8, t_0 = 1$ . Such large values of  $n$  are difficult to consider with the PE as the requirement  $T \gg n!$  may be difficult to achieve in practice. In the simulation

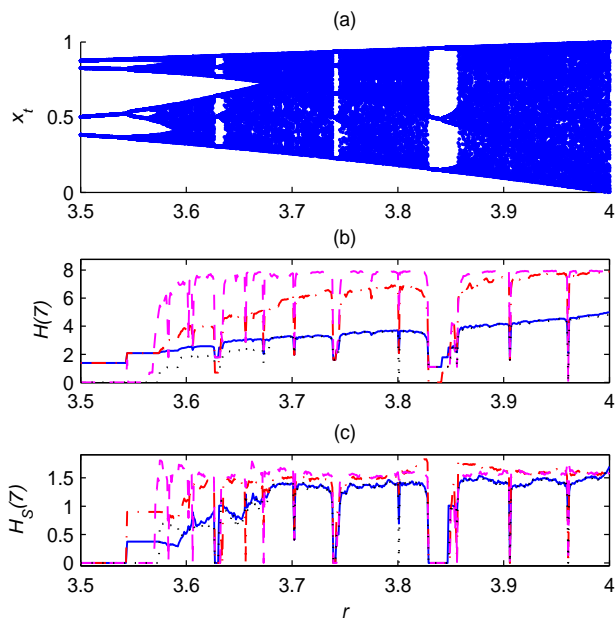


Figure 1: Logistic equation for varying control parameter  $3.5 \leq r \leq 4$  (step  $\Delta r = 10^{-3}$ ),  $T = 5000$ : (a) Bifurcation diagram, (b) PE  $H(7)$  for  $\tau = 1$  and  $t_0 = 1$  (blue solid line),  $\tau = 3$  and  $t_0 = 1$  (red dash-dotted line),  $\tau = 8$  and  $t_0 = 1$  (magenta dashed line) and  $\tau = 1$  and  $t_0 = 8$  (black dotted line); (c) PLSE  $H_S(7)$  for  $\tau = 1$  and  $t_0 = 1$  (blue solid line),  $\tau = 3$  and  $t_0 = 1$  (red dash-dotted line),  $\tau = 8$  and  $t_0 = 1$  (magenta dashed line) and  $\tau = 1$  and  $t_0 = 8$  (black dotted line).

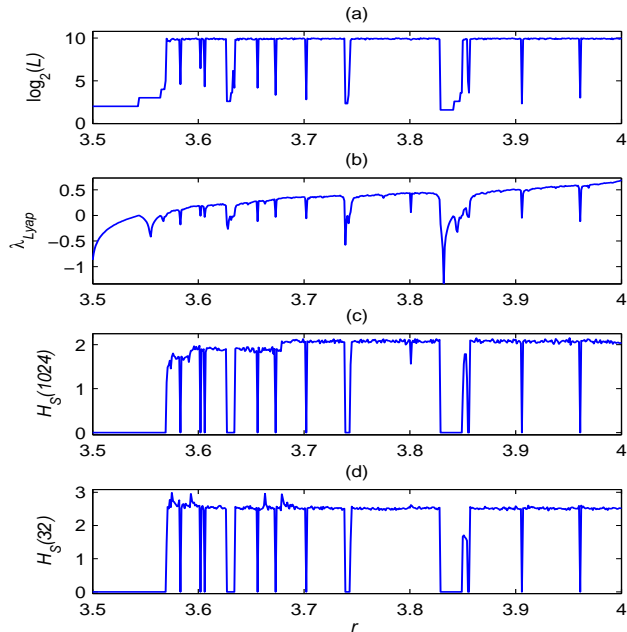


Figure 2: Logistic equation for varying control parameter  $3.5 \leq r \leq 4$  (step  $\Delta r = 10^{-3}$ ),  $T = 5000$ : (a) Cycle diagram for  $\tau = 1$  and  $t_0 = 8$ ; (b) Lyapunov exponent  $\lambda_{Lyap}$ ; (c)  $H_S(1024)$ ,  $\tau = 1$  and  $t_0 = 8$ ; (d)  $H_S(32)$ ,  $\tau = 8$  and  $t_0 = 1$ .

below, the results of the PLSE are compared with the Lyapunov exponent. According to Fig. 2, choosing large values of  $n$  effectively allows to give a better estimate of the periods and to achieve zero entropy even for dynamics with large periods. This result also shows that there is no need to increase the observation time  $T$ , as only three to four cycles of the distinct permutations are required for the dynamics to be detected as periodic. Choosing  $t_0 = 8$  allows to reduce this number of permutations for all regular dynamics whose periods are such that  $\gcd(L, t_0) > 1$  and to reduce the computational time, while choosing  $\tau = 8$  allows to achieve zero PLSE even for period- $L$  cycle dynamics with  $L > 32$  and  $\delta < 32 < L$ . For  $r = 3.602$ , the logistic map exhibits a period-88 cycle dynamics. Considering  $n = 32$  is not enough for detecting this dynamics as periodic. However, combining  $n = 32$  with  $\tau = 8$  allows to obtain  $H_S(32) = 0$  as the 88-periodic orbit is reduced to period- $\delta$  cycle dynamics, with  $\delta = 11$ . Normally, there is a tiny periodic window around  $r = 3.801$  which cannot be clearly observed as  $\Delta r = 0.001$  only. For  $r = 3.801$  the LE is coming close to zero ( $\lambda_{Lyap} = 0.0619$ ), but remains positive. This result is clearly expressed by the PLSE which remains positive even for  $n = 1024$  ( $H_S(1024) = 1.5652$ ), thus confirming the chaotic nature of the corresponding dynamics.

### 3.3. Robustness against noise

The robustness of the PE against noise has already been presented in [1]. In order to verify the efficiency of the PLSE for the detection of regular dynamics in the presence of noise, we have considered the logistic map contaminated

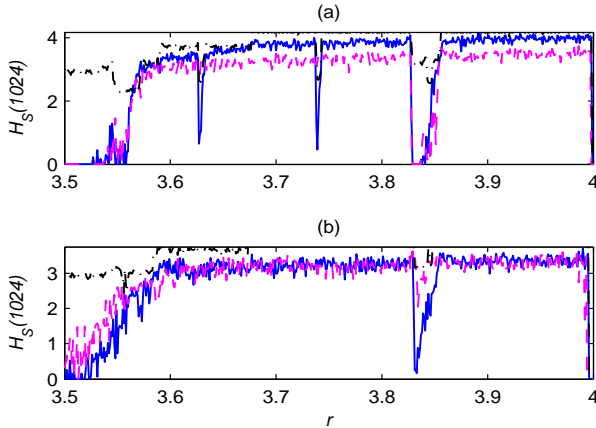


Figure 3: Spectrum of the PLSE for the logistic map in presence of dynamical noise,  $T = 5000$ : (a)  $H_S(1024)$  for the uniform noise,  $\sigma = 0.0005$ ,  $\eta = 0$  (dash-dotted black line),  $\sigma = 0.0005$ ,  $\eta = 3\sigma$  (solid blue line) and  $\sigma = 0.001$ ,  $\eta = 3\sigma$  (dashed magenta line); (b)  $H_S(1024)$  for the Gaussian noise,  $\sigma = 0.0005$ ,  $\eta = 0$  (dash-dotted black line),  $\sigma = 0.0005$ ,  $\eta = 7\sigma$  (solid blue line) and  $\sigma = 0.001$ ,  $\eta = 4\sigma$  (dashed magenta line).

by dynamical and observational noise with Gaussian and uniform distributions whose standard deviations are varying from  $\sigma = 0.0005$  to  $\sigma = 0.005$ . In the case of the dynamical noise, the noisy logistic map is given by:

$$x_{t+1} = rx_t(1 - x_t) + \sigma b_t \quad (9)$$

where  $b_t$  are normally (Gaussian noise) or uniformly (uniform noise) distributed values and  $\sigma$  the standard deviation of the noise. For the observational noise, the noise samples are simply added to the output samples of the logistic map, thus leading to the following equation:

$$\phi_t = x_t + \sigma b_t \quad (10)$$

where  $x_t$  is given by Eq. (8) and  $\phi_t$  the logistic map contaminated by the observational uniform or Gaussian noise  $b_t$ . The noise  $b_t$  is characterized by a standard deviation  $\sigma_0 = 1$  and a mean value  $\overline{b_t} = 0$ . The corresponding Matlab expressions are  $b_t = 4(-0.5 + rand)$  for the uniform noise and  $b_t = randn$  for the Gaussian noise.

The detection results for the dynamical noise are presented in Fig. 3, while those corresponding to the observational noise are shown in Fig. 4.

Figs. 3-4 show that the PLSE performs well in the presence of noise. We use the DDQ with various  $\eta$  for the noise reduction. For  $\eta = 0$ , there is no noise reduction and the corresponding result shows small values of  $H_S$  for some periodic windows, but also large values of  $H_S$  where zero values are expected. Considering  $\eta > 0$  contributes to reinforce the robustness of the PLSE against noise as well as the scaling of chaos. Choosing the right value of  $\eta$  for the noise cancelation remains a difficult task. However, our choice of  $\eta$  is motivated by the amount of noise, so by the standard deviation of the noise. According to the results obtained, the DDQ, combined with the PLSE, appears to be an effective

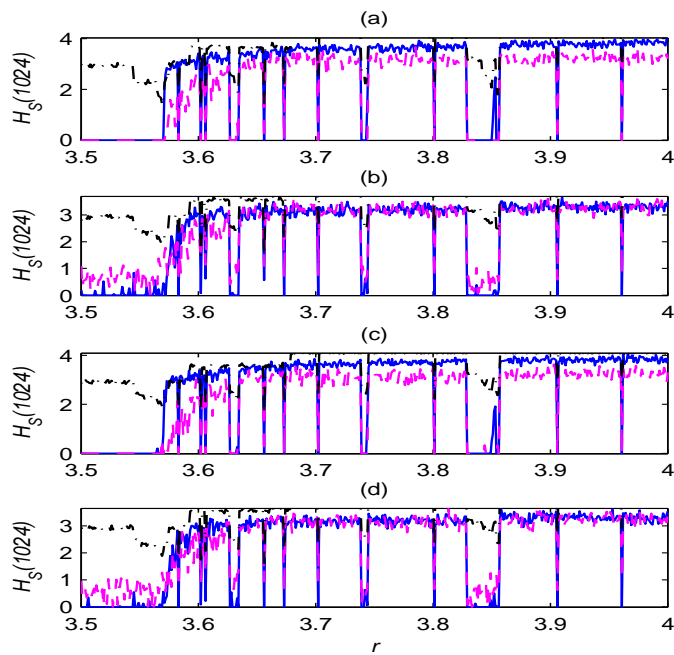


Figure 4: Spectrum of the PLSE ( $H_S(1024)$ ) for the logistic map in presence of observational noise,  $T = 5000$ : (a) case of uniform noise,  $\sigma = 0.0005$ ,  $\eta = 0$  (dash-dotted black line),  $\sigma = 0.0005$ ,  $\eta = \sigma$  (solid blue line) and  $\sigma = 0.001$ ,  $\eta = \sigma$  (dashed magenta line); (b) case of Gaussian noise,  $\sigma = 0.0005$ ,  $\eta = 0$  (dash-dotted black line),  $\sigma = 0.0005$ ,  $\eta = 2\sigma$  (solid blue line) and  $\sigma = 0.001$ ,  $\eta = 2\sigma$  (dashed magenta line); (c) case of uniform noise,  $\sigma = 0.002$ ,  $\eta = 0$  (dash-dotted black line),  $\sigma = 0.002$ ,  $\eta = \sigma$  (solid blue line) and  $\sigma = 0.005$ ,  $\eta = \sigma$  (dashed magenta line); (d) case of Gaussian noise,  $\sigma = 0.002$ ,  $\eta = 0$  (dash-dotted black line),  $\sigma = 0.002$ ,  $\eta = 2\sigma$  (solid blue line) and  $\sigma = 0.005$ ,  $\eta = \sigma$  (dashed magenta line).

approach for noise reduction, especially for the reduction of the observational uniform noise. Such a robustness of the PLSE against noise may be useful for the detection of the regularity from real-world time series.

#### 3.4. Application to continuous time systems

Applying the PE or the PLSE to continuous time series is quite difficult due to the sampling process and the precision of the integrator. Thus, the time series should be considered as noise contaminated. For the PLSE to be efficiently determined, we used the DDQ for noise reduction. We applied the PLSE to the Duffing system described by the following system of ordinary differential equations:

$$\begin{cases} \dot{x} = y \\ \dot{y} = x - ay - x^3 + r \cos(z) \\ \dot{z} = \omega \end{cases} \quad (11)$$

where  $(\dot{\cdot}) = d(\cdot)/dt$ . We used the fourth order Runge-Kutta algorithm to solve Eq. (11) with sampling step  $T_s = 4\pi/1000$ . The algorithm of PLSE is then applied to the solutions  $x_t$  and  $y_t$  and only the maximal value of the corresponding entropies is retained. We consider in the case of PLSE that times series  $\{x_t\}$  and  $\{y_t\}$  are corrupted by a small amount of noise of amplitude  $\varepsilon \leq T_s/10$ , due to sampling and numerical integration. Taking  $\eta = T_s/10$  and applying the DDQ to  $\{x_t\}$  and  $\{y_t\}$ , we obtained the result in Fig. 5(b). Applying the DDQ prior to PE gives approximately the same result as in Fig. 5(c), for which no noise is considered. The result in Fig. 5 shows that the LE  $\lambda_{Lyap}$  and  $h_S(n)$  behave similarly, except for  $r = 0.287$  where  $h_S(n) > 0$  indicates a transition between two stable limit-cycles. This transition is characterized by the detection of two values of largest slopes and can be easily recognized. Fig. 5(c) shows that PE can only detect changes in the dynamics, but cannot give details on their nature. The PLSE algorithm may also be applied to the set of local maxima of  $\{x_t\}$  and  $\{y_t\}$  for obtaining quite the same detection result.

PE accurately estimates the complexity of  $L$ -periodic dynamics iff the conditions  $\gcd(L, \tau) = 1$  and  $\gcd(L, t_0) = 1$  are satisfied. As there is no defined period in the case of non-regular dynamics, such a condition is not required and the PE approximates the complexity of the underlying dynamics better as  $t_0 < n$ .

In contrast, the PLSE always indicates a zero complexity for the regular dynamics whose periods are such that  $L < n$ , as they are perfectly predictable. In the case of non-regular dynamics, the maximum number of distinct permutations is greater than the  $n - 1$  possible values of largest slopes, and the permutations therefore cannot be effectively described by their largest slopes. It then results that the corresponding entropy cannot be considered as a complexity measure. However, as nonzero entropies are supposed to be obtained only for non-regular dynamics and zero entropies for regular dynamics, the PLSE is considered to be a detection entropy. Choosing  $\tau > 1$  allows to reduce detection errors due to small values of embedding dimensions  $n$  while  $1 < t_0 < n$  allows to consider smaller observation time  $T$  for detection purposes. Moreover, choosing  $1 < t_0 < n$  speeds up the scanning time of the time series under study, hence the PLSE algorithm, as the number of embedding vectors analyzed for  $t_0 = 1$  is reduced by a factor of  $t_0$  without error on the detection result. In the sense

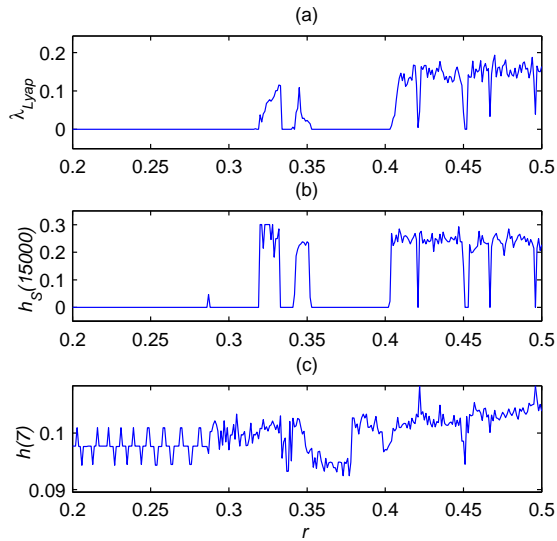


Figure 5: Forced Duffing System for varying control parameter  $0.2 \leq r < 0.5$  (step  $\Delta r = 10^{-3}$ ),  $T = 4 \cdot 10^4$ : (a) Lyapunov exponent, (b)  $h_S(15000)$  and (c)  $h(\bar{7})$ .

of detection, the above results show that the PLSE behaves similar to the positive Lyapunov exponent, whilst outputting zero entropy for regular dynamics without bias.

### 3.5. Application to real-word time series

We considered a real life time series recorded from the low-frequency function generator (FG) presented in Fig. 6(a). This example was preferred to common used time series as it is difficult to find well known regular dynamics in the existing databases. Indeed, the most difficult part is to detect a regular dynamics as regular, given that real life data are noise contaminated. The output signal of the FG was then acquired using the sound card of a 2.6 GHz PC running Windows 8.1, with sampling frequency  $\nu_s = 44100\text{Hz}$ . Data are recorded as double precision values and processed using the PLSE algorithm. The FG is considered as stable as the output signal is regular. The data set under study is inevitably corrupted by the sampling noise, in addition to eventual observational and dynamical noise due to electronic components, power supply fluctuation, etc. The result in Fig. 6(b) is obtained for various values of  $\eta$ . We choose as output of the FG a 2 kHz frequency sine wave signal and the time series analyzed is a 30s recorded data. Each value of  $h_S$  is estimated from a  $T = 22050$ -length frame. The frame overlapping is  $\Delta T = 18050$ . According to the results thus obtained, the time series can be seen as regular as  $\eta \geq 3.5 \cdot 10^{-3}$  or as non-regular for  $\eta < 3.5 \cdot 10^{-3}$ . Considering the time series as regular for  $\eta \geq 3.5 \cdot 10^{-3}$  attests that the underlying real life time series is noise contaminated and that the FG is not rigorously stable: the frequency or the amplitude of the output signal may be fluctuating as the time evolves. This result also suggests that  $\eta$  may be used as an indicator for quantizing the stability of a periodic FG:  $\eta = 0$  indicates a perfectly stable FG.

(a)



(b)

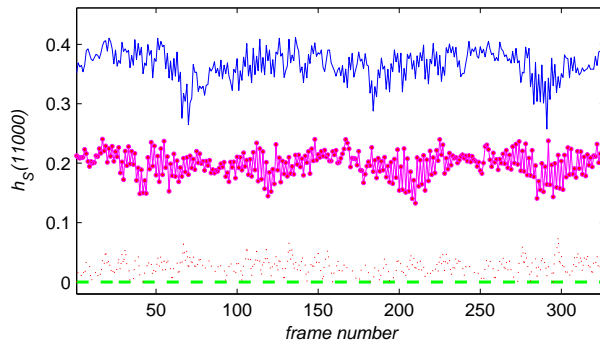


Figure 6: Analysis of an experimental sine wave signal. (a): Function generator used; (b): PLSE results  $h_S(11000)$  for  $\eta = 0$ ,  $\eta = 10^{-3}$ ,  $\eta = 3 \cdot 10^{-3}$  and  $\eta = 4 \cdot 10^{-3}$  from top to bottom.

#### 4. Conclusion

We showed in this paper that the PE estimates the complexity of a regular dynamics with a predictable bias iff  $\gcd(L, \tau) = 1$  and  $\gcd(L, t_0) = 1$ . Otherwise, the PE may take arbitrary values smaller than the predicted bias of the dynamics under investigation, although it should be zero as referred to the KS entropy. In the case of non-regular dynamics, although computing the true entropy requires large embedding dimensions and observation times, so infinitely large memory space, the computed PE approximates the complexity of the underlying dynamics for  $\tau = 1$  and  $t_0 < n$ . In contrast, the PLSE indicates a zero complexity for regular dynamics but cannot efficiently determine the complexity of non-regular dynamics. For  $\tau = 1$  and  $t_0 = 1$ , PE is a good candidate for the complexity measure although it is not well approximating the KS entropy for finite  $n$ , while the PLSE, hence the 3ST, is an effective approach for distinguishing between regular and non-regular dynamics and to detect the phase space period of stable limit cycles. This method allows to achieve zero entropy from observation time  $T$  much smaller than  $n!$ . We also showed that using permutation largest slopes allows to save more computational time, as choosing  $1 < t_0 < n$  does not affect the detection result, nor the estimation of the period of the limit cycles. The results thus obtained in this paper confirm along the way the reliability of the previous results of the 3ST for chaos detection. Note also that the method has been successfully applied to other systems like the sine-circle map, the Henon 2D map and the forced Duffing oscillator, and that the logistic map has been chosen only for illustration due to the length of the paper.

- [1] C. Bandt, B. Pompe, Permutation entropy: A natural complexity measure for time series, *Physical review letters* 88 (2002) 174102.
- [2] J.-P. Eckmann, D. Ruelle, Ergodic theory of chaos, *Rev. Mod. Phys.* 57 (1985) 617.
- [3] Y. B. Pesin, Dimension theory in dynamical systems, Ph.D. thesis, University of Chicago Press, Chicago (1998).
- [4] P. Grassberger, I. Procaccia, Estimation of the kolmogorov entropy from a chaotic signal, *Phys. Rev. A* 28 (1983) 2591–2593.
- [5] M. Ding, C. Grebogi, E. Ott, T. Sauer, J. A. Yorke, Estimating correlation dimension from a chaotic time series: when does it occur?, *Phys. Rev. Lett.* 70 (1993) 3872.
- [6] H. D. I. Abarbanel, *Analysis of Observed Chaotic Data*, Springer, New York, 1996.
- [7] F. Cecconi, M. Cencini, M. Falcioni, A. Vulpiani, Brownian motion and diffusion: from stochastic processes to deterministic chaos, *CHAOS* 15 (2005) 026102.
- [8] O. A. Rosso, H. A. Larrondo, M. T. Martin, A. Plastino, M. A. Fuentes, Distinguishing noise from chaos, *Phys. Rev. Lett.* 99 (2007) 154102.
- [9] J. B. Gao, J. Hu, W. W. Tung, , Y. H. Cao, Distinguishing chaos from noise by scale-dependent lyapunov exponent, *Phys. Rev. E* 74 (2006) 066204.

- [10] A. A. Brudno, Entropy and complexity of the trajectories of a dynamical system, *Trans. Moscow Math. Soc.* 2 (1983) 127–151.
- [11] S. Galatolo, Orbit complexity and data compression, *Discr. Cont. Dyn. Systems* 7 (2001) 477–486.
- [12] S. M. Pincus, Approximate entropy as a measure of system complexity, *Proc. Natl. Acad. Sci.* 88 (1991) 2297–2301.
- [13] S. M. Pincus, A. L. Goldberger, Physiological time series analysis -what does regularity quantify, *Am. J. Physiol. Heart Circ. Physiol.* 266 (1994) 1643–1656.
- [14] B.-L. Hao, Symbolic dynamics and characterization of complexity, *Physica D* 51 (1991) 161–176.
- [15] Z. Li, G. Ouyang, D. Li, X. Li, Characterization of the causality between spike trains with permutation conditional mutual information, *Phys. Rev. E* 84 (2011) 021929.
- [16] X. Li, S. Cui, L. Voss, Using permutation entropy to measure the electroencephalographic effects of sevoflurane, *Anesthesiology* 109 (2008) 448–456.
- [17] X. Li, G. Ouyang, D. Richards, Predictability analysis of absence seizures with permutation entropy, *Epilepsy Res.* 77 (2007) 70–74.
- [18] A. Bruzzo, B. Gesierich, M. Santi, C. Tassinari, N. Bir-baumer, G. Rubboli, Permutation entropy to detect vigilance changes and preictal states from scalp eeg in epileptic patients: a preliminary study, *Neurol. Sci.* 29 (2008) 3–9.
- [19] Y. Cao, W. Tung, J. Gao, V. Protopopescu, L. Hively, Detecting dynamical changes in time series using the permutation entropy, *Phys. Rev. E* 70 (2004) 046217.
- [20] J. M. Amigó, *Permutation complexity in dynamical systems*, Springer, 2010.
- [21] B. Fadlallah, J. Príncipe, B. Chen, A. Keil, Weighted-permutation entropy: An improved complexity measure for time series, *Phys. Rev. E* 87 (2013) 022911.
- [22] C. Bian, C. Qin, Q. D. Y. Ma, Q. Shen, Modified permutation-entropy analysis of heartbeat dynamics, *Phys. Rev. E* 85 (2012) 021906.
- [23] V. A. Unakafova, K. Keller, Efficiently measuring complexity on the basis of real-world data, *Entropy* 15 (2013) 4392–4415.
- [24] V. A. Unakafov, K. Keller, Conditional entropy of ordinal patterns, *Physica D* 269 (2014) 94–102.
- [25] G. A. Gottwald, I. Melbourne, A new test for chaos in deterministic systems, *Proc. Roy. Soc. London. Ser. A* 460 (2004) 603611.
- [26] G. A. Gottwald, I. Melbourne, On the implementation of the 0-1 test for chaos, *SIAM J. Appl. Dyn. Syst.* 8 (2009) 129145.

- [27] G. A. Gottwald, I. Melbourne, On the validity of the 0-1 test for chaos, *Nonlinearity* 22 (2009) 1367.
- [28] R. Gopal, A. Venkatesan, M. Lakshmanan, Applicability of 0-1 test for strange nonchaotic attractors., *CHAOS* 23 (2013) 023123.
- [29] J. S. A. E. Fouda, B. Bodo, S. L. Sabat, J. Y. Effa, A modified 0-1 test for chaos detection in oversampled time series observations, *IJBC* 24 (2014) 1450063.
- [30] J. S. A. E. Fouda, J. Y. Effa, M. Kom, M. Ali, The three-state test for chaos detection in discrete maps, *Applied Soft Computing* 13 (2013) 4731–4737.
- [31] J. S. A. E. Fouda, W. Koepf, Efficient detection of the quasi-periodic route to chaos by the three-state test, *Nonlinear Dyn.* DOI 10.1007/s11071-014-1529-4.
- [32] P. Collet, J.-P. Eckmann, *Iterated Maps on the Interval as Dynamical Systems*, Birkhaeuser, Basel, 1980.